Published in final edited form as:
Sci Signal. ; 5(225): ra38. doi:10.1126/scisignal.2002767.

IFNβ therapy against EAE is effective only when development of the disease depends on the NLRP3 inflammasome

Makoto Inoue[1], **Kristi L. Williams**[2], **Timothy Oliver**[3], **Peter Vandenabeele**[4,5], **Jayant V. Rajan**[6,7], **Edward A. Miao**[8], and **Mari L. Shinohara**[1,9]

[1]Department of Immunology, Duke University Medical Center, Durham, NC 27710, USA

[2]Departments of Medicine and Cardiology, Duke University Medical Center, Durham, NC 27710, USA

[3]Department of Cell Biology, Duke University Medical Center, Durham, NC 27710, USA

[4]Department for Molecular Biomedical Research, Vlaams Instituut voor Biotechnologie (VIB), 9052 Ghent (Zwijnaarde), Belgium

[5]Department of Biomedical Molecular Biology, Ghent University, 9052 Ghent (Zwijnaarde), Belgium

[6]Institute for Systems Biology, Seattle, WA 98103, USA

[7]Department of Medicine, University of Washington, Seattle, WA 98195, USA

[8]Department of Microbiology and Immunology, University of North Carolina, Chapel Hill, NC 27599, USA

[9]Department of Molecular Genetics and Microbiology, Duke University Medical Center, Durham, NC 27710, USA

Abstract

Interferon-β (IFN-β) is widely used to treat multiple sclerosis (MS), and its efficacy was demonstrated in the setting of experimental autoimmune encephalomyelitis (EAE), an animal model of MS; however, IFN-β is not effective in treating all cases of MS. Here, we demonstrate that signaling by IFNAR (the shared receptor for IFN-α and IFN-β) on macrophages inhibits activation of Rac1 and the generation of reactive oxygen species (ROS) through suppressor of cytokine signaling 1 (SOCS1). The inhibition of Rac1 activation and ROS generation suppressed the activity of the NLRP3 inflammasome, which resulted in attenuated EAE pathogenicity. We further found that two subsets of EAE could be defined on the basis of their dependency on the NLRP3 inflammasome and that IFN-β was not an effective therapy when EAE was induced in an NLRP3 inflammasome–independent fashion. Thus, our study demonstrates a previously uncharacterized signaling pathway that is involved in the suppression of EAE by IFN-β and characterizes NLRP3-independent EAE, which cannot be treated with IFN-β.

INTRODUCTION

Type 1 interferons (IFNs), such as IFN-α and IFN-β, are involved in various aspects of immune responses and the pathogenesis of various diseases. For example, IFN-β has been used for more than 15 years as a first-line treatment for multiple sclerosis (MS). Study of an animal model of MS, experimental autoimmune encephalomyelitis (EAE), has contributed

Corresponding Author: Mari L. Shinohara, PhD, Department of Immunology, DUMC-3010, Duke University Medical Center, Durham 27710, U.S.A., Tel: 919-613-6977, Fax: 919-684-8982, mari.shinohara@duke.edu.

to our understanding of the pathogenesis of MS, and three approved MS medications have been directly developed from studies of EAE (1). Using the EAE model, we and another group have shown that the inhibitory effect of IFN-β is mediated by innate immune cells, such as macrophages and dendritic cells (DCs), which inhibit T helper 17 (TH17) responses through interleukin-27 (IL-27) (2, 3). Other studies also demonstrated that type I IFNs ameliorate EAE by reducing antigen presentation, inhibiting the proliferation of T cells, altering the abundance of matrix metalloproteases, and altering cytokine responses through signaling by the type I IFN receptor (IFNAR) in myeloid cells (4–6). Despite such basic knowledge, the mechanisms of the occasional failure in IFN-β therapy are not clear. Previous studies showed that IFN-β suppresses the production of IL-1β (7, 8). IL-1β production is achieved in two steps. First, receptors [such as Toll-like receptor 4 (TLR4) ligation by lipopolysaccharide (LPS)], and then pro–IL-1β is processed by inflammasomes to form mature IL-1β (9). The Nod-like receptor (NLR) family, pyrin domain–containing 3 (NLRP3) inflammasome, on which we focus in this study, is a cytoplasmic sensor that is activated by various pathogens and damage-associated molecules, including extracellular adenosine triphosphate (ATP), nigericin, and monosodium urate (MSU) (9–12). How IFNAR signaling represses the NLRP3 inflammasome was not clear except that signal transducer and activator of transcription 1 (STAT1), a major downstream molecule of IFNAR, mediates the signaling (8).

Here, we showed that IFN-β is effective only when EAE is developed in an NLRP3 inflammasome–dependent fashion. First, we demonstrated that type I IFNs inhibit activation of the NLRP3 inflammasome in macrophages by decreasing the abundance of active Rac1 through a mechanism involving suppressor of cytokine signaling 1 (SOCS1). Rac1 is a small G protein and a member of the Rac subfamily of the Rho family of guanosine triphosphatases GTPases, which are involved in various cellular activities, such as cytoskeletal reorganization, control of cell growth, and the activation of protein kinases. Here, we demonstrated that IFNAR signaling induces SOCS1-mediated ubiquitination and degradation of active Rac1. Reduction of active Rac1 decreased the production of mitochondrial reactive oxygen species (ROS), resulting in inhibition of NLRP3 inflammasome activity. Second, we showed that EAE could develop independently of the NLRP3 inflammasome and that such NLRP3 inflammasome–independent EAE does not respond to IFN-β.

RESULTS

IFNAR signaling inhibits production of IL-1β

Activation of IFNAR signaling in innate immune cells results in various physiological consequences. To identify the function of IFNAR signaling in innate immune cells, we compared macrophages from wild-type mice and *Ifnar1*$^{-/-}$ mice. Because previous studies have shown that IFNAR signaling is constitutively activated by low amounts of endogenous type I IFNs, both in vivo and ex vivo (13, 14), the altered phenotypes of *Ifnar1*$^{-/-}$ cells should be detected without adding exogenous type I IFN. We found that compared to wild-type macrophages, *Ifnar1*$^{-/-}$ macrophages produced increased amounts of IL-1β upon stimulation with LPS (see Materials and Methods) and ATP (Fig. 1A). In turn, under the same conditions, recombinant IFN-α (rIFN-α) or rIFN-β suppressed the production of IL-1β by wild-type macrophages (fig. S1, A to C). We also observed suppression of IL-1β production by IFNAR signaling when cells were treated with either nigericin or MSU (which activates the NLRP3 inflammasome) combined with LPS (9) (fig. S1, D to I). In addition, rIFN-α suppressed the production of IL-18, another cytokine that is processed by the NLRP3 inflammasome (fig. S1J). In contrast, IFNAR signaling did not inhibit IL-1β production by macrophages stimulated with Salmonella typhimurium (fig. S1K), which

activates the NLRC4 inflammasome (15). These results suggested that IFNAR signaling inhibited cytokine production mediated by the NLRP3 inflammasome.

Activation of the NLRP3 inflammasome is inhibited by IFNAR signaling

We then tested whether deficiency in IFNAR impaired the production of pro–IL-1β by LPS; however, the amounts of Il1b mRNA and pro–IL-1β protein were not increased in LPS-treated Ifnar1$^{-/-}$ macrophages compared to those in LPS-treated wild-type macrophages (fig. S2, A and B). Although we cannot rule out an indirect effect of type I IFN on the production of pro–IL-1β at later time points, these results prompted us to investigate the mechanism of the direct suppressive effect of IFNAR signaling on the NLRP3 inflammasome. We first evaluated NLRP3 inflammasome activity by measuring the amount of caspase-1 p20, which reflects activated caspase-1 and the NLRP3 inflammasome, and we found that the amount of p20 was increased in *Ifnar1*$^{-/-}$ macrophages compared to that in wild-type macrophages (Fig. 1B). We also investigated whether *Ifnar1*$^{-/-}$ macrophages showed increased oligomerization of the NLRP3 inflammasome complex by measuring the numbers, stained areas, and intensity of caspase-1 foci, because the NLRP3 inflammasome must oligomerize to be activated (16). ATP induced foci formation in wild-type and *Ifnar1*$^{-/-}$ cells; however, quantitative analysis of confocal images showed that foci in *Ifnar1*$^{-/-}$ cells were larger, more frequent, and had more staining intensity than those in wild-type cells (Fig. 1, C and D). In agreement with this result, rIFN-α reduced the frequency and intensity of foci formation in wild-type cells (fig. S3). In summary, our data suggested that IFNAR signaling inhibited the activity of the NLRP3 inflammasome.

IFNAR signaling inhibits the generation of mitochondrial ROS

Next, we tried to identify the mechanism by which IFNAR signaling suppresses NLRP3 inflammasome activity. We first examined the expression of the genes Nlrp3, Asc, and Casp1, which encode components of the NLRP3 inflammasome, but we found no difference in their expression when we compared wild-type and *Ifnar1*$^{-/-}$ macrophages (fig. S4A). We also found no alteration in the expression of Txnip (fig. S4A), which encodes thioredoxin-interacting protein, which interacts with NLRP3 and participates in the activation of the NLRP3 inflammasome (17). Because ATP activates the NLRP3 inflammasome, we then evaluated the cell surface abundances of the ATP receptor P2X7R (9) and CD39, an ectonucleotidase that hydrolyzes extracellular ATP (18); however, we found that they were also not altered in *Ifnar1*$^{-/-}$ cells (fig. S4B). Next, we asked whether IFNAR signaling inhibited the generation of molecules that activate the NLRP3 inflammasome. A major activator of the NLRP3 inflammasome is ROS (19). We detected increased amounts of ROS in *Ifnar1*$^{-/-}$ macrophages compared to those in wild-type macrophages after stimulation with ATP (fig. S4C). Treatment with rIFN-a accordingly dampened ATP-induced ROS generation in wild-type cells (Fig. 2A). These data suggested that IFNAR signaling suppressed the generation of ROS generation. Mitochondria are considered to be the major source of ROS that activate the NLRP3 inflammasome (20), but NADPH (reduced form of nicotinamide adenine dinucleotide phosphate) oxidase also produces ROS. To confirm that the treatment of cells with ATP induces ROS production from mitochondria, we measured ROS generation with MitoSOX Red, an indicator of mitochondrial superoxide. We found that the amount of mitochondrial ROS produced 30 min after stimulation with ATP was maximal (fig. S5A). Treatment of macrophages with rIFN-α or rIFN-β suppressed the generation of mitochondrial ROS 30 min after stimulation with ATP (fig. S5B). On the other hand, the involvement of NADPH oxidase in IFN-β–mediated suppression of ROS was negligible because we found no obvious inhibition of ROS generation or IL-1β production in macrophages deficient in p47phox, a key component of NADPH oxidase (fig. S5, C and D).

An inhibitor of Rac1 suppresses the generation of ROS

Mitochondrial generation of ROS is induced by Rac1 (21), a member of the Rho family of GTPases. We first confirmed that the generation of ROS and IL-1β by ATP was suppressed by the Rac1 inhibitor NSC23766 in a dose-dependent manner (Fig. 2B and fig. S6, A and B). We further ruled out a global effect of Rac1 inhibition on cytokine production by showing that NSC23766 did not alter the abundances of Il1b, Tnfa, and Il6 mRNAs (fig. S6C) or the amounts of tumor necrosis factor–α (TNF-α) and IL-6 proteins (fig. S6D). Collectively, these data suggested that inhibition of Rac1 inhibited ROS generation, which led to inhibition of NLRP3 inflammasome activation and decreased IL-1β generation.

IFNAR signaling inhibits Rac1 activation by SOCS1-mediated suppression of Vav1 and Rac1-GTP

We observed that the stimulation of cells with ATP activated Rac1 but that the addition of IFN-β prevented Rac1 activation, as determined by the measurement of the amount of Rac1 bound to GTP (Rac1-GTP), the active form of Rac1 (Fig. 2C). This result suggested that IFN-β inhibited the activation of Rac1. Here, we found that the treatment of macrophages with IFN-β resulted in reduced amounts of Vav1 protein, a guanine nucleotide exchange factor (GEF) for Rac1 (fig. S7A), which suggested that Vav1 mediated the suppression of Rac1 activation by IFN-β. Because SOCS1 mediates the degradation of Vav through ubiquitination (22), we asked whether the suppression of Vav1 by IFN-β was mediated by SOCS1. We found that IFNAR signaling induced Socs1 expression (Fig. 3A) and that silencing of Socs1 mRNA with short hairpin RNA (shRNA) derepressed Vav1 expression in wild-type macrophages (fig. S7B). These results suggested that IFNAR signaling suppresses Vav1 through SOCS1. We also confirmed the efficacy of Socs1 silencing with shRNA (fig. S7C). In addition, we found that SOCS1 directly suppressed Rac1-GTP by ubiquitin-mediated degradation, as determined by coimmunoprecipitation of Rac1-GTP and SOCS1 (Fig. 3B and fig. S7D) and by the detection of the substantial ubiquitination ofRac1-GTP (Fig. 3C). We found that derepression of Rac1-GTP and ROS generation was observed in cells in which Socs1was silenced (Fig. 3, D and E). Furthermore, inhibition of IL-1β production by IFN-β was partially reversed by silencing Socs1 (fig. S7E). Next, we asked whether the NLRP3 inflammasome itself had a feedback effect on the abundances of SOCS1, Vav1, Rac1-GTP, and ROS. First, we confirmed the failure of events downstream of the NLRP3 inflammasome, such as caspase-1 activation and IL-1β generation, in *Nlrp3*$^{-/-}$ macrophages and *Asc*$^{-/-}$ macrophages (fig. S8, A and B). On the other hand, the abundances of SOCS1, Vav1, and Rac1-GTP and the generation of ROS were unchanged in *Nlrp3*$^{-/-}$ and *Asc*$^{-/-}$ macrophages compared to those in wild-type macrophages (fig. S8, C to G). These results suggested that molecules upstream of the NLRP3 inflammasome, including SOCS1, Vav1, Rac1-GTP, and ROS, were regulated by IFNAR signaling and not by the feedback effect of impaired or suppressed activity of the NLRP3 inflammasome. In summary, IFNAR signaling induced SOCS1 activity, which inhibited Rac1 activation, ROS generation, and eventually NLRP3 inflammasome activity (Fig. 3F).

EAE progression is induced by active NLRP3 inflammasome

Next, we sought to delineate the activation status of the NLRP3 inflammasome during EAE progression. We found that whereas wild-type mice developed EAE, *Asc*$^{-/-}$ and *Nlrp3*$^{-/-}$ mice did not (Fig. 4A). In wild-type mice with EAE, we detected a consistent increase in the amount of serum IL-1β from day 0 to day 17 (disease peak) (Fig. 4B). This increase in systemic IL-1β abundance in wild-type mice was entirely dependent on the NLRP3 inflammasome because IL-1β was undetectable in *Asc*$^{-/-}$ and *Nlrp3*$^{-/-}$ mice (Fig. 4B). Similarly, increased amounts of serum IL-18 were observed in wild-type mice, but not in *Asc*$^{-/-}$ and *Nlrp3*$^{-/-}$ mice, on day 9 (fig. S9). We also evaluated NLRP3 inflammasome activity in mice by measuring the ability of splenocytes to exhibit IL-1β maturation. This

was achieved by stimulating splenocytes with LPS alone, which induces the production of pro–IL-1β but cannot activate the NLRP3 inflammasome. Splenocytes obtained on day 9 from immunized wild-type mice produced IL-1β upon stimulation with LPS (Fig. 4C), suggesting that the NLRP3 inflammasome in splenocytes of immunized wild-type mice was active. We also confirmed activation of the NLRP3 inflammasome by detecting caspase-1 p20 in wild-type splenocytes on day 9 after EAE induction (Fig. 4D).

IFN-β suppresses NLRP3 inflammasome activity and ameliorates EAE

We next asked whether IFN-β suppressed NLRP3 inflammasome activity in mice with EAE. First, we confirmed the ex vivo efficacy of rIFN-β to induce expression of Socs1 and of IFN-stimulated genes, such as Ip10 (Cxcl10) and Mx1, in macrophages (fig. S10). The efficacy of rIFN-β in vivo was demonstrated by the amelioration of EAE (Fig. 4E). As expected, rIFN-β reduced the amounts of serum IL-1β, the production of IL-1β by splenocytes, and the generation of caspase-1 p20 protein in splenocytes (Fig. 4, F to H). Consistent with these results, these parameters were increased in *Ifnar1*$^{-/-}$ mice compared to those in wild-type mice (fig. S11). Collectively, these data suggest that rIFN-β suppresses the NLRP3 inflammasome to ameliorate EAE.

Aggressive immunization induces a form of EAE that does not respond to IFN-β

We showed that either the lack of the NLRP3 inflammasome or the treatment with rIFN-β protected mice from EAE; however, this situation still does not reflect the full complexity observed in MS patients, one-third of whom fail to respond to IFN-β. In the EAE model (Fig. 4), a mouse was injected with MOG (myelin oligodendrocyte glycoprotein) peptide in complete Freund's adjuvant (CFA) that contained 200 mg of heat-killed Mycobacteria (Mtb), and a deficiency in NLRP3 or ASC protected mice from EAE. However, aggressive immunization regimens induced EAE in *Nlrp3*$^{-/-}$ and *Asc*$^{-/-}$ mice in a manner that depended on the dose of Mtb. We observed considerably severe EAE symptoms in *Nlrp3*$^{-/-}$ and *Asc*$^{-/-}$ mice injected with 300 mg or more of Mtb, but no EAE in mice injected with 200 mg of Mtb (fig. S12). We then induced EAE in wild-type, *Nlrp3*$^{-/-}$ and *Asc*$^{-/-}$ mice with 300 mg of Mtb and asked whether IFN-β ameliorated EAE. We found that IFN-β was not effective against EAE in the *Nlrp3*$^{-/-}$ and *Asc*$^{-/-}$ mice, which have a defective NLRP3 inflammasome (Fig. 5, B and C). These findings suggested that the IFN-β treatment is not effective when EAE progression is independent of the NLRP3 inflammasome.

Passive EAE induces NLRP3 inflammasome activation and can be treated by IFN-β

Mtb induces NLRP3 inflammasome activation (23). Therefore, we sought to delineate whether the NLRP3 inflammasome is activated in EAE induced without CFA. To induce passive EAE, we isolated CD4+ T cells from immunized mice and then intravenously transferred them to naïve *Rag2*$^{-/-}$ and *Rag2*$^{-/-}$*Nlrp3*$^{-/-}$ mice (Fig. 6A). *Rag2*$^{-/-}$ mice lack T cells and B cells and are often used as T cell hosts in the induction of passive EAE. *Rag2*$^{-/-}$ recipients developed EAE, but *Rag2*$^{-/-}$ *Nlrp3*$^{-/-}$ recipients did not (Fig. 6B), suggesting that the passive EAE model was NLRP3 inflammasome–dependent. We next asked whether the passive EAE model activated the NLRP3 inflammasome and whether IFN-β suppressed its activity to ameliorate passive EAE. We confirmed the activation of the NLRP3 inflammasome in *Rag2*$^{-/-}$ recipients, but not in *Rag2*$^{-/-}$*Nlrp3*$^{-/-}$ recipients, by detecting IL-1β in the serum, measuring the ability of splenocytes to produce mature IL-1β, and by detecting caspase-1 p20 (Fig. 6, C to E). In the spleen, macrophages in particular showed the ability to induce the maturation of IL-1β (fig. S13). *Rag2*$^{-/-}$ recipients showed a substantial response to IFN-β by ameliorating EAE (Fig. 6B), together with the inhibition of NLRP3 inflammasome activity (Fig. 6, C to E). We further observed that cells that had infiltrated the brain in the context of passive EAE had the ability to induce IL-1β maturation (fig. S13), suggesting that the NLRP3 inflammasome was activated in the brain as well as in the spleen.

Together, these data suggest that theNLRP3 inflammasome can be activated in EAE induced without CFA and that such EAE is ameliorated by treatment with IFN-β.

DISCUSSION

Here, we report two findings: First, that a suppressive mechanism of IFN-β on NLRP3 inflammasome activity is mediated by SOCS1, Vav1, Rac1-GTP, and the generation of mitochondrial ROS generation, and second, that EAE can be divided into two subsets on the basis of their dependency on the NLRP3 inflammasome; the NLRP3 independent form of EAE cannot be treated with IFN-β.

Two studies showed that IFN-β suppresses IL-1β production (7, 8). One of the studies showed that IL-27 mediates the inhibition of IL-1β production by IFN-β but did not investigate the inhibitory mechanism of IL-27 (7). A possible mechanism by which IL-1β production is suppressed by IL-27 is through the targeting of the first step of pro– IL-1β generation by IL-27 receptor (IL-27R) signaling. In the study (7), cells were stimulated with zymosan, which activates theNLRP3 inflammasome through signaling by the receptor dectin-1 and the kinase Syk (24, 25). Therefore, the zymosan-activatedNLRP3 inflammasome is poised to process pro–IL-1β in this experimental system, but if IL-27R signaling targets the production of pro–IL- 1b, then the scarce supply of pro–IL-1β would inhibit the generation of IL-1β.

The second possibility is that IL-27R signaling targets the maturation of IL-1β by interfering with the dectin-1–Syk–NLRP3 axis to inhibit the NLRP3 inflammasome (24, 25). If this is the case, it will be of interest to determine whether IL-27 suppresses NLRP3 inflammasome activation that is triggered by ATP. Whether Syk-mediated NLRP3 inflammasome activity occurs during EAE progression is also an interesting question. Another study showed that the autocrine effect of IL-10 mediates the suppression of pro–IL-1β production in response to IFN-β, that is, by targeting the first step in pro–IL-1β generation (8). We did not observe suppression of pro–IL-1β production by macrophages that had been preincubated for 24 hours with IFN-β before being stimulated for 3 hours with LPS. The same group also showed suppression of NLRP3 inflammasome activity by IFN-β, whereby signal transducer and activator of transcription 1 (STAT1), which signals downstream of IFNAR, mediated the suppressive role (8). However, how IFNAR signaling inhibits NLRP3 inflammasome activity was not described in that report; therefore, it is still unclear whether suppression of NLRP3 inflammasome activated by alum and Candida, which are used in that study, is mediated by the same pathway that we identified here. These previous studies and ours suggest the presence of multiple mechanisms to inhibit IL-1β production. Because IL-1β is a potent proinflammatory molecule that has a substantial effect on immunity, multiple layers of mechanisms to suppress IL-1β may have been developed during evolution as protection against excessive inflammation.

The intensity of the EAE-induction regimen determines the phenotypes of EAE. Two reports described EAE in *Nlrp3*$^{-/-}$ mice, one of which concluded that NLRP3 plays a critical role (26), whereas the other concluded that NLRP3 is not involved in the progression of EAE (27). It appears that the EAE-induction regimens used were different in both reports. In particular, aggressive EAE induction seems to have been performed in the study showing that *Nlrp3*$^{-/-}$ mice develop severe EAE (27). The results from both reports may appear to be conflicting, but we assume that the two distinct results reflect two different subtypes of EAE. We showed that immunization with 300 mg of Mtb in CFA induced EAE in *Asc*$^{-/-}$ *and Nlrp3*$^{-/-}$ mice, whereas immunization with 200 mg of Mtb in CFA failed to do so. As a result of immunization with 300 mg of Mtb, wild-type mice developed slightly more severe EAE than did *Asc*$^{-/-}$ *and Nlrp3*$^{-/-}$ mice (Fig. 5). This is probably because the intensity of

immunization still enabled wild-type mice to develop NLRP3 inflammasome–dependent EAE in addition to NLRP3 inflammasome–independent EAE. Indeed, in wild-type mice, IFN-β was only partially efficacious in treating EAE induced with 300 mg of Mtb compared to its effects on EAE induced with 200 mg of Mtb. As for *Asc*$^{-/-}$ *and Nlrp3*$^{-/-}$ mice, it is possible that even more intensive induction of EAE, for example, with 300 to 400 mg of Mtb, is required to develop EAE that is as severe as that observed in wild-type mice. Although the efficacy of IFN-β was not tested, a similar phenomenon was observed in a study of caspase-1–deficient mice, which do not develop EAE when immunized with a low dose of antigenic peptide but do develop EAE with increased antigen dosage (28). Therefore, it appears that intensive antigen presentation to T cells induces EAE in an NLRP3 inflammasome–independent fashion.

We showed that a subtype of EAE, which did not respond to IFN-β, could be induced by aggressive immunization. Stromnes et al. reported "atypical EAE," which was induced in major histocompatibility complex (MHC) congenic C3H mice (29). Such atypical EAE was characterized by severe disease progression and an enhanced ratio of TH17 cells to TH1 cells in the central nervous system (29). The authors also demonstrated that the high TH17/TH1 ratio correlated with the functional avidity of the antigenic peptide for MHC (29). Atypical EAE, described in the study, may have similarities with EAE induced by aggressive immunization (and that is NLRP3 inflammasome–independent) in terms of intense T cell stimulation. Although the efficacy of IFN-β was not evaluated in the study of atypical EAE, Axtell et al. showed that TH17-induced EAE cannot be treated by IFN-β (30). At this point, it is not known whether the findings of Stromnes et al. (29) and Axtell et al. (30) can be connected to ours. To do so, one must ask the following questions: Is atypical EAE NLRP3 inflammasome–independent and does it not respond to IFN-β, and is NLRP3 inflammasome–independent EAE prone to develop a high TH17/TH1 ratio?

We are currently addressing why aggressive disease induction regimens can induce EAE independently of the NLRP3 inflammasome. It is also important to elucidate the role of the NLRP3 inflammasome in MS and to understand whether those patients who do not respond to IFN-β therapy are those who have MS that developed in an NLRP3 inflammasome–independent manner. A number of reports strongly suggest the involvement of inflammasomes in the development of MS. For example, Furlan et al. showed the involvement of caspase-1, a key component of inflammasomes, in MS (31), and Ming et al. showed that caspase-1 was highly abundant in MS plaques (32). Huang et al. further demonstrated the increased abundance of caspase-1 and IL-18 in peripheral mononuclear cells from MS patients compared to those in cells from healthy controls (33). Therefore, we suggest that it is likely that the NLRP3 inflammasome is involved in the pathogenicity of MS. Here, we speculated that events in MS that are equivalent to aggressive immunization might be severe infections or even severe sterile inflammation. In conclusion, we have demonstrated a previously uncharacterized signaling pathway in which activation of the NLRP3 inflammasome is inhibited by IFN-β, and we described a subset of EAE that does not respond to IFN-β therapy. These findings may be a first step to exploring the possibility of a new prognostic approach for the treatment of MS.

MATERIALS AND METHODS

Animals

Male mice of the C57BL/6 background were used in this study. *Ifnar1*$^{-/-}$ mice were backcrossed to C57BL/6 mice for 12 generations. The *Asc*$^{-/-}$ *and Nlrp3*$^{-/-}$ mice were a gift from Genentech and were rederived in our facility. C57BL/6 and 2D2 T cell receptor (TCR) transgenic (Tg) mice were purchased from Jackson Laboratories. All of the mice were kept

in a barrier facility. This study was approved by the Duke University Institutional Animal Care and Use Committee.

Reagents, antibodies, and recombinant proteins

Ultrapure LPS (InvivoGen), which is highly purified LPS that does not activate inflammasomes, was used throughout this study instead of regular LPS. ATP (used at a final concentration of 5 mM unless otherwise noted) and nigericin were purchased from Sigma-Aldrich. NSC23766 was purchased from Calbiochem. Antibody against caspase-1 p10 for immunocytochemistry was purchased from Santa Cruz. Antibodies against Rac1 and Rac1-GTP were from Millipore and New East Biosciences, respectively. Antibodies against Vav1 and ubiquitin were purchased from Cell Signaling. Mouse rIFN-α and rIFN-β were purchased from Hycult and PBL, respectively. The rIFN-β used in the treatment of EAE was human rIFN-β-1b (Betaseron). MOG35–55 peptide was synthesized by New England Peptides. Enzyme-linked immunosorbent assay (ELISA) kits for the detection of IL-1β, TNF, and IL-6 were purchased from BD PharMingen, and an ELISA kit for IL-18 was purchased from Bender MedSystems.

Cell isolation and culture

Peritoneal macrophages were elicited by injection of mice with thioglycollate. Bone marrow macrophages (BMMs) were derived by culturing bone marrow cells with L929 cell supernatant. To detect NLRP3 inflammasome activity in splenocytes, we used ELISA to measure IL-1β production by splenocytes, which were stimulated with Ultrapure LPS (100 ng/ml) for 24 hours. In the experiment, Opti-MEM medium was used for the cell culture. We used complete RPMI medium unless otherwise noted. RNA and complementary DNA preparation and qPCR analysis Total RNA was extracted from cells with TRIzol (Invitrogen). Complementary DNA (cDNA) synthesis was performed with qScript cDNA SuperMix (Quanta). Real-time, quantitative polymerase chain reaction (qPCR) analysis was performed with KAPA SYBR FAST (Kapa Bio Systems) on the MyiQ PCR System (Bio-Rad) with an initial denaturing step at 95°C for 3 min followed by 45 cycles of a denaturation step at 94°C for 3 s and an annealing and extension step at 60°C for 30 s. The relative amounts of qPCR products were determined with the DDCt method to compare the relative expression of target genes and housekeeping genes. The expression of the gene encoding b-actin was used as an internal control (34). Primer sequences can be found in table S1.

Pull-down assays, immunoprecipitations, and Western blotting analysis

Rac1 activity was evaluated by performing a pull-down assay with the Rac1/Cdc42 activation assay kit (Millipore) as indicated by the supplier. To evaluate the physical association between SOCS1 and Rac1-GTP, we performed coimmunoprecipitation experiments with an antibody against Rac1-GTP and then used an antibody against SOCS1 to detect SOCS1 protein by Western blotting. To detect caspase-1 p20, we cultured peritoneal macrophage or BMMs (5 × 106 cells) in Opti-MEM medium and treated them with Ultrapure LPS (100 ng/ml) for 3 hours and then with 5 mM ATP for an additional hour. To detect Vav1, we analyzed lysates from BMMs (5 × 106 cells) by Western blotting with antibody against Vav1 (1:1000). Horseradish peroxidase (HRP)–conjugated secondary antibody (1:1000, BD Pharmingen) was used to detect signals, which were visualized by enhanced chemiluminescence (ECL, Amersham Pharmacia Biotech).

Analysis of caspase-1 foci formation

To activate caspase-1 (that is, the NLRP3 inflammasome), we incubated macrophages with ATP for 30 min at 37°C. In some experiments, cells were treated with rIFN-α for 24 hours

before ATP treatment. Cells were stained with anti–caspase-1 p10 antibody. After the confocal microscopic images of cells were captured, the frequency (%) of caspase-1–positive focus formation was calculated by enumerating the number of cells within a group of 100 cells that had formed distinct caspase-1–positive foci. The integrated fluorescence intensity was determined from at least 10 caspase-1–positive cells by digitally calculating the pixel-to-pixel fluorescence intensity of caspase-1 staining. Statistical analysis was performed on the results from four mice. Background was defined as the fluorescence intensity in the cytoplasmic areas without caspase-1 focus formation.

Detection of ROS production

BMMs were stimulated with ATP for 30 min at 37°C before being harvested. In some experiments, cells were pretreated with rIFN-β or NSC23766 (Rac1 inhibitor) for 24 hours before being treated with ATP. ROS was detected by flow cytometry with either 2.5 mM dihydroethidium (DHE, Biotium), 5 mM CM-H2DCFDA (Molecular Probes), or 5 mM MitoSOX Red (Molecular Probes), which were added at same time as ATP.

Silencing SOCS1 with Socs1-specific shRNA

Cells were transfected with Socs1-specific shRNA or control shRNA expression vectors (Santa Cruz). Four hours after transfection, cells were treated with rIFN-β for 24 hours. To detect Rac1 activation or ROS generation, we added ATP for the last 10 or 30 min, respectively.

Induction and evaluation of EAE

EAE induction was performed as previously described (2). Briefly, MOG35–55 peptide (100 mg per mouse) was emulsified with CFA (100 ml per mouse, including 200 mg of Mtb) and subcutaneously injected into the flanks of mice on day 0. Mice were also intraperitoneally injected with pertussis toxin (200 ng per mouse) on days 0 and 2. Mice were assessed daily for clinical signs of EAE in a blinded fashion. In some experiments, we used higher dosages of Mtb in CFA (100 ml per mouse, including indicated Mtb). To induce passive EAE, we isolated CD4+ T cells from the spleens and lymph nodes of 2D2 TCR Tg mice 9 days after MOG immunization and adoptively transferred them by intravenous injection into *Rag2*$^{-/-}$ or *Rag2*$^{-/-}$*Nlrp3*$^{-/-}$ recipient mice (2.5 × 106 cells per mouse). EAE scores were evaluated on the basis of the following criteria: 1, tail limpness; 2, impaired righting reflex; 3, hindlimb paralysis; 4, hind- and forelimb paralysis; 5, death.

Statistical analysis

Statistical analysis was evaluated with Student's t tests or one-way analysis of variance (ANOVA) analysis with the Tukey-Kramer method. The criterion of significance was set as $P < 0.05$. All results are expressed as the means ± SEM.

Supplementary Material

Refer to Web version on PubMed Central for supplementary material.

Acknowledgments

We thank G. Kelsoe, T. Tedder, M. Krangel, D. Gunn, C. Gordy, and K. Kobayashi for critical discussions and reading of the manuscript. Funding: This study was funded by the National Multiple Sclerosis Society (RG4536-A-1) to M.L.S., the NIH (AI089756) to K.L.W., and a Methusalem grant from the Flemish government (BOF09/01M00709) to P.V. Author contributions: M.I. and M.L.S. designed the study, analyzed the data, and wrote the manuscript; M.I. performed most of the experiments; K.L.W. and P.V. contributed critical reagents and discussed the data; T.O. contributed microscope analyses; J.V.R. performed the experiments with S. typhimurium and p47 phox-deficient cells; and E.A.M. analyzed the data. Competing interests: M.I. and M.L.S. have applied for

a patent (US #13/347,233) based on this work. Data and materials availability: Use of the *Nlrp3*$^{-/-}$ and *Asc*$^{-/-}$ mice requires the signing of a materials transfer agreement (MTA).

References

1. Denic A, Johnson AJ, Bieber AJ, Warrington AE, Rodriguez M, Pirko I. The relevance of animal models in multiple sclerosis research. Pathophysiology. 2011; 18:21–29. [PubMed: 20537877]
2. Shinohara ML, Kim JH, Garcia VA, Cantor H. Engagement of the type I interferon receptor on dendritic cells inhibits T helper 17 cell development: Role of intracellular osteopontin. Immunity. 2008; 29:68–78. [PubMed: 18619869]
3. Guo B, Chang EY, Cheng G. The type I IFN induction pathway constrains Th17- mediated autoimmune inflammation in mice. J Clin Invest. 2008; 118:1680–1690. [PubMed: 18382764]
4. Hartung HP, Bar-Or A, Zoukos Y. What do we know about the mechanism of action of disease-modifying treatments in MS? J Neurol. 2004; 251(suppl 5):v12–v29. [PubMed: 15549350]
5. Markowitz CE. Interferon-b: Mechanism of action and dosing issues. Neurology. 2007; 68:S8–S11. [PubMed: 17562848]
6. Prinz M, Schmidt H, Mildner A, Knobeloch KP, Hanisch UK, Raasch J, Merkler D, Detje C, Gutcher I, Mages J, Lang R, Martin R, Gold R, Becher B, Bruck W, Kalinke U. Distinct and nonredundant in vivo functions of IFNAR on myeloid cells limit autoimmunity in the central nervous system. Immunity. 2008; 28:675–686. [PubMed: 18424188]
7. Sweeney CM, Lonergan R, Basdeo SA, Kinsella K, Dungan LS, Higgins SC, Kelly PJ, Costelloe L, Tubridy N, Mills KH, Fletcher JM. IL-27 mediates the response to IFN-β therapy in multiple sclerosis patients by inhibiting Th17 cells. Brain Behav Immun. 2011; 25:1170–1181. [PubMed: 21420486]
8. Guarda G, Braun M, Staehli F, Tardivel A, Mattmann C, Förster I, Farlik M, Decker T, Du Pasquier RA, Romero P, Tschopp J. Type I interferon inhibits interleukin-1 production and inflammasome activation. Immunity. 2011; 34:213–223. [PubMed: 21349431]
9. Mariathasan S, Weiss DS, Newton K, McBride J, O'Rourke K, Roose-Girma M, Lee WP, Weinrauch Y, Monack DM, Dixit VM. Cryopyrin activates the inflammasome in response to toxins and ATP. Nature. 2006; 440:228–232. [PubMed: 16407890]
10. Gross O, Poeck H, Bscheider M, Dostert C, Hannesschläger N, Endres S, Hartmann G, Tardivel A, Schweighoffer E, Tybulewicz V, Mocsai A, Tschopp J, Ruland J. Syk kinase signalling couples to the Nlrp3 inflammasome for anti-fungal host defence. Nature. 2009; 459:433–436. [PubMed: 19339971]
11. Martinon F, Petrilli V, Mayor A, Tardivel A, Tschopp J. Gout-associated uric acid crystals activate the NALP3 inflammasome. Nature. 2006; 440:237–241. [PubMed: 16407889]
12. Halle A, Hornung V, Petzold GC, Stewart CR, Monks BG, Reinheckel T, Fitzgerald KA, Latz E, Moore KJ, Golenbock DT. The NALP3 inflammasome is involved in the innate immune response to amyloid-b. Nat Immunol. 2008; 9:857–865. [PubMed: 18604209]
13. Taniguchi T, Takaoka A. A weak signal for strong responses: Interferon-a/b revisited. Nat Rev Mol Cell Biol. 2001; 2:378–386. [PubMed: 11331912]
14. Gresser I. Biologic effects of interferons. J Invest Dermatol. 1990; 95:66S–71S. [PubMed: 1701811]
15. Miao EA, Leaf IA, Treuting PM, Mao DP, Dors M, Sarkar A, Warren SE, Wewers MD, Aderem A. Caspase-1-induced pyroptosis is an innate immune effector mechanism against intracellular bacteria. Nat Immunol. 2010; 11:1136–1142. [PubMed: 21057511]
16. Martinon F, Mayor A, Tschopp J. The inflammasomes: Guardians of the body. Annu Rev Immunol. 2009; 27:229–265. [PubMed: 19302040]
17. Zhou R, Tardivel A, Thorens B, Choi I, Tschopp J. Thioredoxin-interacting protein links oxidative stress to inflammasome activation. Nat Immunol. 2010; 11:136–140. [PubMed: 20023662]
18. Kaczmarek E, Koziak K, Sévigny J, Siegel JB, Anrather J, Beaudoin AR, Bach FH, Robson SC. Identification and characterization of CD39/vascular ATP diphosphohydrolase. J Biol Chem. 1996; 271:33116–33122. [PubMed: 8955160]

19. Tschopp J, Schroder K. NLRP3 inflammasome activation: The convergence of multiple signalling pathways on ROS production? Nat Rev Immunol. 2010; 10:210–215. [PubMed: 20168318]
20. Zhou R, Yazdi AS, Menu P, Tschopp J. A role for mitochondria in NLRP3 inflammasome activation. Nature. 2011; 469:221–225. [PubMed: 21124315]
21. Murthy S, Ryan A, He C, Mallampalli RK, Carter AB. Rac1-mediated mitochondrial H2O2 generation regulates MMP-9 gene expression in macrophages via inhibition of SP-1 and AP-1. J Biol Chem. 2010; 285:25062–25073. [PubMed: 20529870]
22. De Sepulveda P, Ilangumaran S, Rottapel R. Suppressor of cytokine signaling-1 inhibits VAV function through protein degradation. J Biol Chem. 2000; 275:14005–14008. [PubMed: 10747851]
23. Dorhoi A, Nouailles G, Jörg S, Hagens K, Heinemann E, Pradl L, Oberbeck-Müller D, Duque-Correa MA, Reece ST, Ruland J, Brosch R, Tschopp J, Gross O, Kaufmann SH. Activation of the NLRP3 inflammasome by Mycobacterium tuberculosis is uncoupled from susceptibility to active tuberculosis. Eur J Immunol. 2012; 42:374–384. [PubMed: 22101787]
24. Kumar H, Kumagai Y, Tsuchida T, Koenig PA, Satoh T, Guo Z, Jang MH, Saitoh T, Akira S, Kawai T. Involvement of the NLRP3 inflammasome in innate and humoral adaptive immune responses to fungal b-glucan. J Immunol. 2009; 183:8061–8067. [PubMed: 20007575]
25. Kankkunen P, Teirila L, Rintahaka J, Alenius H, Wolff H, Matikainen S. (1,3)-b- Glucans activate both dectin-1 and NLRP3 inflammasome in human macrophages. J Immunol. 2010; 184:6335–6342. [PubMed: 20421639]
26. Gris D, Ye Z, Iocca HA, Wen H, Craven RR, Gris P, Huang M, Schneider M, Miller SD, Ting JP. NLRP3 plays a critical role in the development of experimental autoimmune encephalomyelitis by mediating Th1 and Th17 responses. J Immunol. 2010; 185:974–981. [PubMed: 20574004]
27. Shaw PJ, Lukens JR, Burns S, Chi H, McGargill MA, Kanneganti TD. Cutting edge: Critical role for PYCARD/ASC in the development of experimental autoimmune encephalomyelitis. J Immunol. 2010; 184:4610–4614. [PubMed: 20368281]
28. Furlan R, Martino G, Galbiati F, Poliani PL, Smiroldo S, Bergami A, Desina G, Comi G, Flavell R, Su MS, Adorini L. Caspase-1 regulates the inflammatory process leading to autoimmune demyelination. J Immunol. 1999; 163:2403–2409. [PubMed: 10452974]
29. Stromnes IM, Cerretti LM, Liggitt D, Harris RA, Goverman JM. Differential regulation of central nervous system autoimmunity by TH1 and TH17 cells. Nat Med. 2008; 14:337–342. [PubMed: 18278054]
30. Axtell RC, de Jong BA, Boniface K, van der Voort LF, Bhat R, De Sarno P, Naves R, Han M, Zhong F, Castellanos JG, Mair R, Christakos A, Kolkowitz I, Katz L, Killestein J, Polman CH, deWaal Malefyt R, Steinman L, Raman C. T helper type 1 and 17 cells determine efficacy of interferon-b in multiple sclerosis and experimental encephalomyelitis. Nat Med. 2010; 16:406–412. [PubMed: 20348925]
31. Furlan R, Filippi M, Bergami A, Rocca MA, Martinelli V, Poliani PL, Grimaldi LM, Desina G, Comi G, Martino G. Peripheral levels of caspase-1 mRNA correlate with disease activity in patients with multiple sclerosis; a preliminary study. J Neurol Neurosurg Psychiatry. 1999; 67:785–788. [PubMed: 10567499]
32. Ming X, Li W, Maeda Y, Blumberg B, Raval S, Cook SD, Dowling PC. Caspase-1 expression in multiple sclerosis plaques and cultured glial cells. J Neurol Sci. 2002; 197:9–18. [PubMed: 11997061]
33. Huang WX, Huang P, Hillert J. Increased expression of caspase-1 and interleukin-18 in peripheral blood mononuclear cells in patients with multiple sclerosis. Mult Scler. 2004; 10:482–487. [PubMed: 15471361]
34. Shinohara ML, Lu L, Bu J, Werneck MB, Kobayashi KS, Glimcher LH, Cantor H. Osteopontin expression is essential for interferon a production by plasmacytoid dendritic cells. Nat Immunol. 2006; 7:498–506. [PubMed: 16604075]

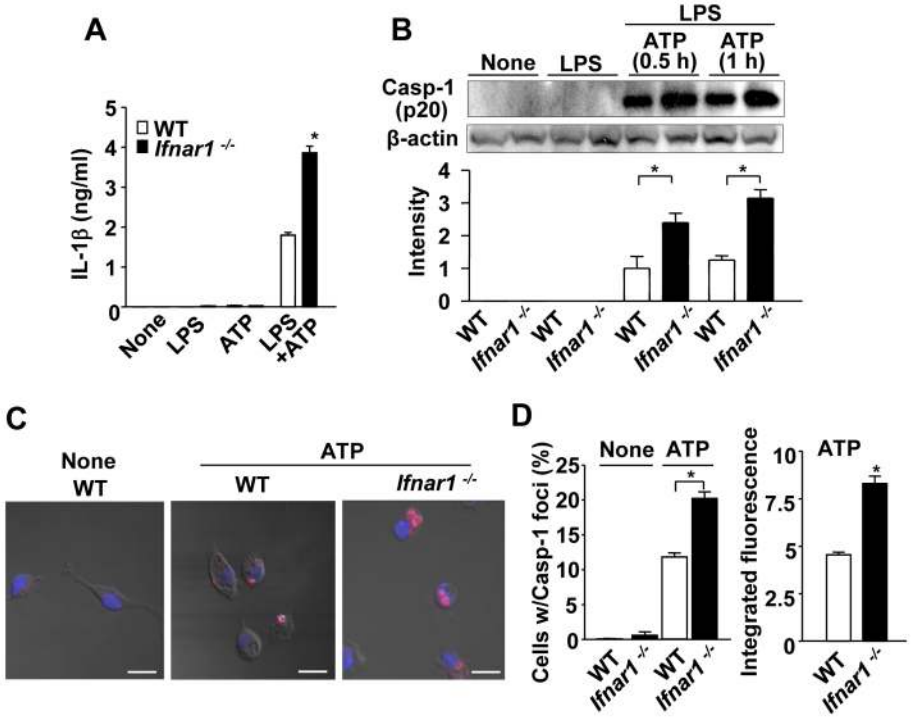

Fig. 1.

IFNAR signaling suppresses activation of the NLRP3 inflammasome. (**A**) Wild-type (WT) and *Ifnar1*$^{-/-}$ peritoneal macrophages were incubated for 3.5 hours with LPS alone (100 ng/ml), 5 mM ATP alone, or a combination of LPS and ATP (ATP was added for the last 30 min), and the amount of IL -1β produced was measured. Representative data from three independent experiments are shown. Data are the mean ± SEM from four mice. (**B**) *Ifnar1*$^{-/-}$ macrophages exhibit increased amounts of active caspase-1 (Casp-1 p20). Cells were incubated with or without LPS (100 ng/ml) for 3.5 h with ATP added for the last 30 or 60 min. Casp-1 p20 and β actin proteins were detected by Western blotting analysis of cell culture supernatants and cell lysates, respectively. Western blots are representative of three independent experiments. Densitometric analysis of pooled experiments are shown in the bar graph. (**C**) Representative confocal microscopic images of caspase -1 (red) and DAPI (blue) staining in WT and *Ifnar*$^{-/-}$ macrophages. Macrophages were incubated with or without 5 mM ATP for 30 min at 37°C. Scale bar: 10 μm. Data are the mean ± SEM from four experiments. (**D**) Frequencies of caspase -1 foci and integrated fluorescence intensities (combined measure of staining area and intensity) of foci in WT and *Ifnar1*$^{-/-}$ macrophages. Data are the mean ± SEM from four mice. *$P < 0.05$.

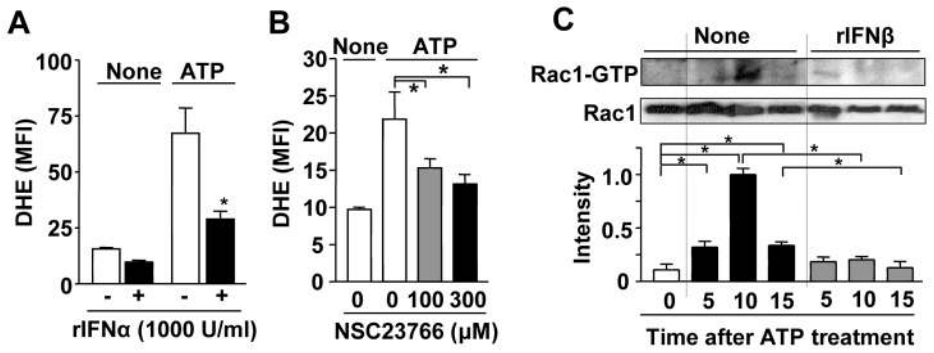

Fig. 2.

IFNAR signaling suppresses Rac1-GTP. (**A, B**) ROS generation was evaluated by detecting dihydroethidium (DHE) by flow cytometry. Data are the mean ± SEM from four experiments. WT BMMs were treated with or with out rIFNα (1000 U/ml) for 24 hours, with 5 mM ATP added for the last 30 min (A). Cells were pretreated with NSC23766 at the indicated concentration s 24 h ours before treatment with ATP (B). (**C**) BMMs were pretreated with IFN β (1000 U/ml) for 24 h ours before being treated with ATP for the indicated times. Rac1-GTP was detected by Western blotting. Blots are representative of four independent experiments. Densitometric analysis of the abundance of Rac1-GTP normalized to that of total Rac1 from the four experiments is shown in the bar graph. The sample that had the greatest amount of Rac1-GTP was set at a relative intensity value of 1.

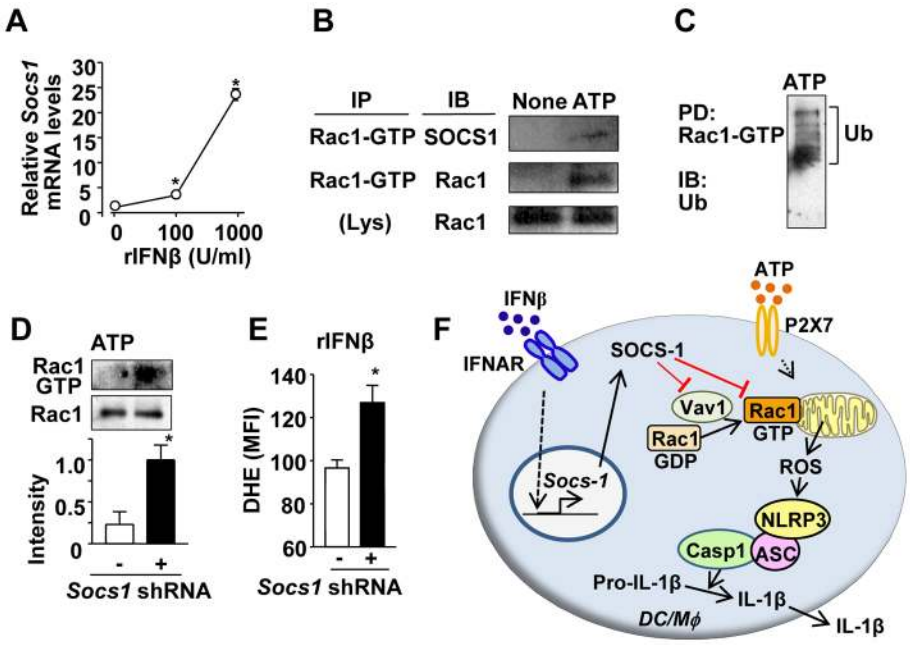

Fig. 3.

SOCS1 mediates the IFNAR-dependent suppression of Rac1 activation and ROS generation. (**A**) Measurement of the relative abundance of *Socs-1* mRNA in BMMs treated for 6 hours with rIFNβ at the indicated concentrations. Data are the mean ± SEM from four experiments. (**B**) Coimmunoprecipitation of Rac1-GTP and SOCS1 in BMMs 10 min after treatment with ATP. Samples were subjected to immunoprecipitation (IP) with antibody against Rac1-GTP and were analyzed by Western blotting (IB) with antibody against SCOS1. (**C**) Ubiquitination was detected in a Rac1-GTP pull-down fraction obtained from cells lysed 10 min after treatment with ATP. Samples were analyzed by Western blotting with an antibody against ubiquitin. Data in (B) and (C) are representative of three independent experiments. (**D** and **E**) *Socs1* silencing derepresses the extent of (D) Rac1 activation (statistics from three independent experiments) and (E) ROS generation in BMMs. Cells were transfected with plasmids encoding *Socs1*-specific shRNA (+) or control shRNA (–). Four hours later, cells were treated with rIFNβ for 24 hours and stimulated with ATP for the last 10 min. The Western blot in (D) is representative of three independent experiments, and densitometric analysis of all experiments are shown in the bar graph. Data shown in (E) are the mean ± SEM from four experiments. (**F**) Schematic model for type I IFN mediated inhibition of the NLRP3 inflammasome through SOCS1-mediated inhibition of ROS generation. $*P < 0.05$.

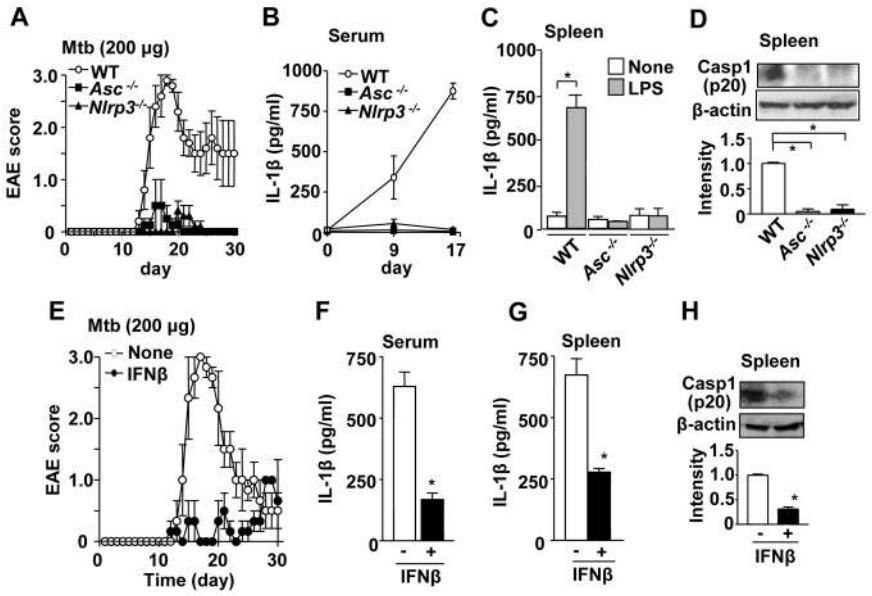

Fig. 4.

IFNβ ameliorates EAE by suppressing NLRP3 inflammasome activity. (**A**) EAE was induced and scored in WT, *Asc*$^{-/-}$, and *Nlrp3*$^{-/-}$ mice as described in the Materials and Methods. Data are from three independent experiments. (**B**) Serum IL-1β concentrations in mice on the indicated days after EAE induction. (**C**) Splenocytes were isolated from mice 9 days after EAE induction, and were then treated in vitro with LPS for 24 hours. The amount of IL-1β in the culture supernatant was determined by ELISA. (**D**) Detection of caspase-1 p20 in splenocyte culture supernatant 24 hours after cells were plated without stimulation. β-actin was detected in corresponding cell lysates. Western blots are representative of five independent experiments, and densitometric analysis of all experiments is shown in the bar graph. (**E** to **H**) EAE was induced in (E) WT mice, as described for (A), and mice were treated intraperitoneally with or without rIFN β (3×10^4 unit/mouse) on every other day from day 0 to 10. IL -1β concentrations in (F) serum and (G) culture supernatants of splenocytes, which were treated as described for (C), are shown from mice 9 days after induction of EAE. (H) Caspase-1 p20 was detected by Western blotting analysis of splenocytes from mice 9 days after induction of EAE in four independent experiments. Data shown are the mean ± SEM of 5 mice for each group, unless otherwise noted. *$P < 0.05$.

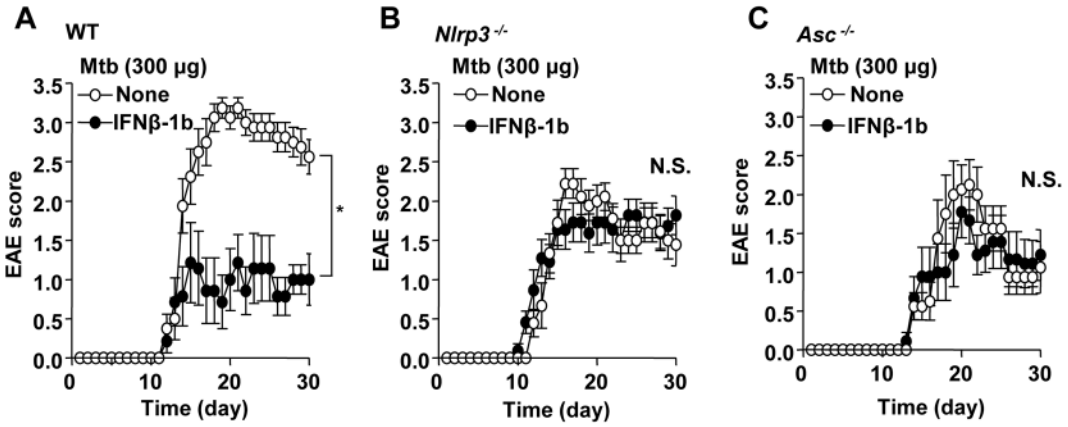

Fig. 5.

rIFNβ ameliorates the severity of EAE, but only when disease progression is mediated by the NLRP3 inflammasome. (**A** to **C**) EAE was induced with CFA including 300 μg of Mtb. (A) WT, (B) *Nlrp3*$^{-/-}$, and (C) *Asc*$^{-/-}$ mice were treated intraperitoneally with rIFNβ (3×10^4 unit/mouse) every other day from day 0 to day 10 after induction of EAE. Disease scores are presented as the mean ± SEM for each group (*n=4* to *6* mice). Data are representative of at least two independent experiments. *$P < 0.05$. N. S., not significant.

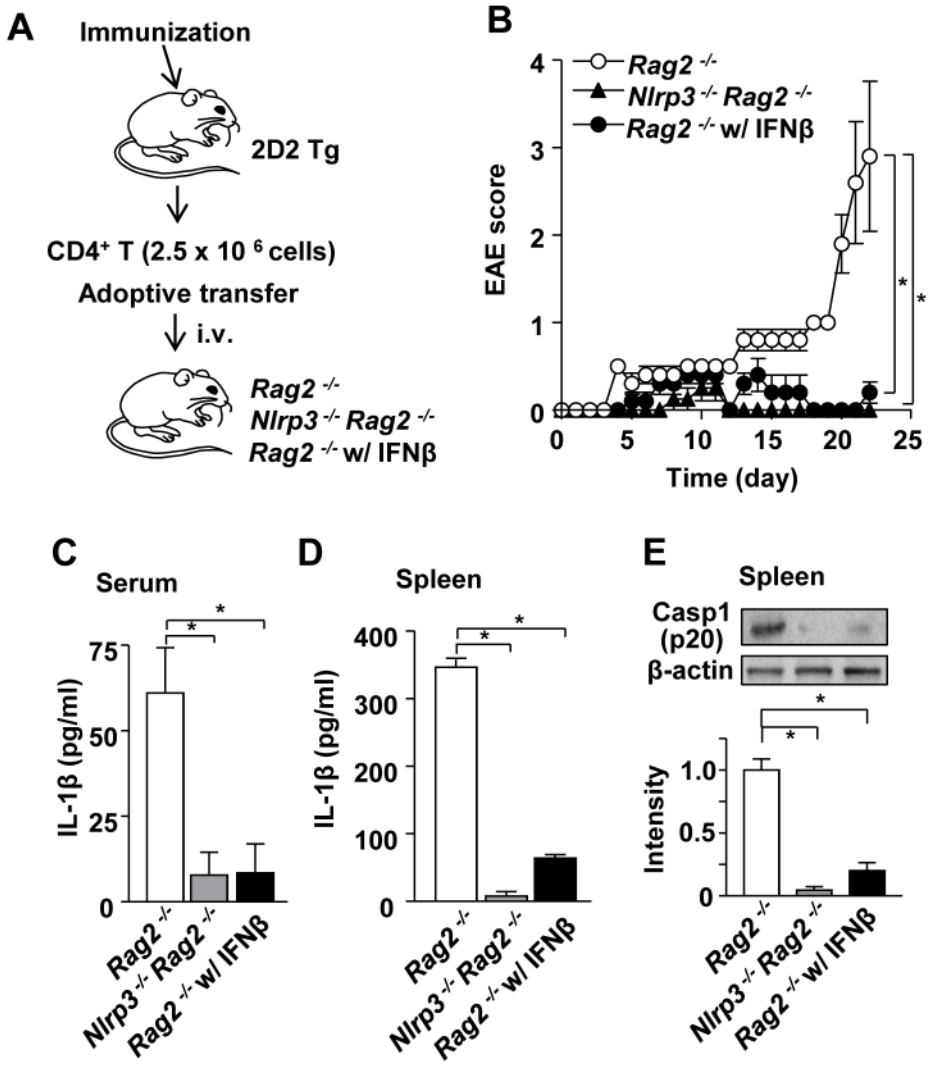

Fig. 6.

Passive EAE develops in an NLRP3 inflammasome dependent fashion and responds to IFNβ. (**A**) Schematic procedure for the induction of passive EAE. $CD4^+$ T cells were obtained from immunized 2D2 TCR Tg mice and were transferred to *Rag2*$^{-/-}$ or *Rag2*$^{-/-}$ *Nlrp3*$^{-/-}$ recipient mice. Some *Rag2*$^{-/-}$ mice were treated intraperitoneally with rIFNβ (3×10^4 unit/mouse) every third day between day 0 and day 15 after adoptive transfer of the T cells. (**B**) Development of passive EAE. Disease scores are presented as the mean ± SEM for each group ($n = 4$ to 5 mice). (**C**) IL-1β concentrations in serum on day 23 after T cell transfer. (**D**) IL-1β production by splenocytes stimulated with LPS in vitro. (**E**) Detection of caspase-1 p20 in splenocytes isolated from *Rag2*$^{-/-}$ mice that were untreated or were treated with rIFNβ, and from *Rag2*$^{-/-}$ *Nlrp3*$^{-/-}$ mice. Data are the mean ± SEM from three experiments unless otherwise noted. $^*P < 0.05$.